Fundamental limitations for polarization estimation with applications in array signal processing

Nordebo, Sven; Gustafsson, Mats; Lundbäck, Jonas

2005

CODEN:LUTEDX/(TEAT-7137)/1-14/(2005)

Fundamental Limitations for Polarization Estimation with Applications in Array Signal Processing

Sven Nordebo, Mats Gustafsson, and Jonas Lundbäck

Department of Electroscience
Electromagnetic Theory
Lund Institute of Technology
Sweden

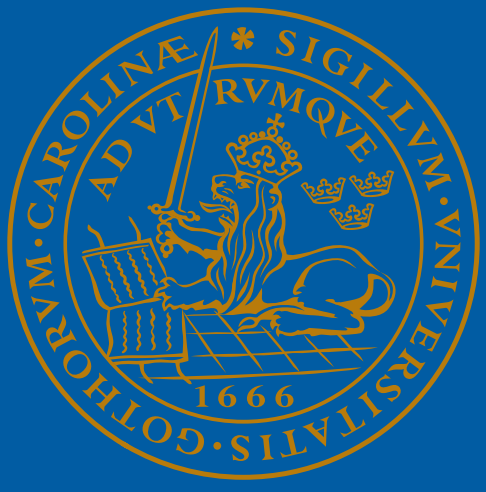

Sven Nordebo
Sven.Nordebo@msi.vxu.se

School of Mathematics and Systems Engineering
Växjö University
351 95 Växjö
Sweden

Mats Gustafsson
Mats.Gustafsson@es.lth.se

Department of Electroscience
Electromagnetic Theory
Lund Institute of Technology
P.O. Box 118
SE-221 00 Lund
Sweden

Jonas Lundbäck
Jonas.Lundback@msi.vxu.se

School of Mathematics and Systems Engineering
Växjö University
351 95 Växjö
Sweden

Editor: Gerhard Kristensson

Abstract

In this paper we demonstrate that the combination of statistical signal processing, electromagnetic theory and antenna theory yields simple and very useful tools for analyzing fundamental physical limitations associated with polarization and/or DOA estimation using arbitrary multiport antennas. By using spherical vector modes as a generic model for the scattering, we show how the corresponding Cramer-Rao lower bounds can be calculated for any real antenna system. The spherical vector modes and their associated equivalent circuits and Q factor approximations are used together with the broadband Fano theory as a general framework for analyzing electrically small multiport antennas. Finally, we employ a principal parameter analysis based on the SVD of the Fisher information matrix to evaluate the performance of an ideal multimode antenna processor with respect to its ability to estimate the state of polarization of a partially polarized plane wave coming from a given direction.

1 Introduction

The Direction of Arrival (DOA) estimation using antenna arrays has been the topic for research in array and statistical signal processing over several decades and comprises now well developed modern techniques such as maximum likelihood and subspace methods, see e.g. [19, 27, 31] and the references therein. Recently, there has been an increased interest in incorporating properties of electromagnetic wave propagation with the statistical signal estimation techniques used for sensor array processing and there are several papers dealing with direction finding and polarization estimation using electromagnetic vector sensors and diversely polarized antenna arrays, tripole arrays, etc., see e.g. [11–14, 20, 21, 28, 32–35].

The classical theory of radiation Q uses spherical vector modes and equivalent circuits to analyze the properties of a hypothetical antenna inside a sphere, see e.g. [2, 3, 6, 7, 9, 10, 22, 29]. An antenna with a high Q factor has electromagnetic fields with large amounts of stored energy around it, and hence, typically low bandwidth and high losses [9]. From a radiation point of view, the high-order vector modes give the high-resolution aspects of the radiation pattern. As is well known, any attempt to accomplish supergain will result in high currents and near fields, thereby setting a practical limit to the gain available from an antenna of a given size, see also [17]. The classical theory of broadband matching shows how much power that can be transmitted between a transmission line and a given load [5], i.e. the antenna. Hence, by considering an antenna of a given size and bandwidth, together with the Q factors which are computable for each vector mode [3], the broadband Fano-theory [5] can be used to estimate the maximum useful multipole order, and to calculate an upper bound for the transmission coefficient of any particular vector mode, see also [8, 25, 26].

In this paper we show how the Cramer-Rao lower bounds for DOA and/or polarization estimation can be derived for arbitrary multiport antennas by using spherical vector modes as a generic model for the scattering. In particular, by using the classical theory of radiation Q together with the broadband Fano theory, we evaluate

the performance of an ideal multimode antenna processor with respect to its ability to estimate the state of polarization of a partially polarized plane wave coming from a given direction.

2 Signal Model for Receiving Antennas

2.1 Spherical Vector Waves, Radiation Q and Broadband Fano Theory

Assume that all sources are contained inside a sphere of radius $r = a$, and let $k = \omega/c$ denote the wave number, $\omega = 2\pi f$ the angular frequency, $\mathrm{e}^{\mathrm{i}\omega t}$ the time-convention, and c and η the speed of light and the wave impedance of free space, respectively. The transmitted electric and magnetic fields, $\boldsymbol{E}(\boldsymbol{r})$ and $\boldsymbol{H}(\boldsymbol{r})$, can then be expanded in *outgoing spherical vector waves* $\boldsymbol{u}_{\tau ml}(k\boldsymbol{r})$ for $r > a$ as [1, 15, 24]

$$\boldsymbol{E}(\boldsymbol{r}) = \sum_{l=1}^{\infty}\sum_{m=-l}^{l}\sum_{\tau=1}^{2} f_{\tau ml}\boldsymbol{u}_{\tau ml}(k\boldsymbol{r}) \tag{2.1}$$

$$\boldsymbol{H}(\boldsymbol{r}) = -\frac{1}{\mathrm{i}\eta}\sum_{l=1}^{\infty}\sum_{m=-l}^{l}\sum_{\tau=1}^{2} f_{\tau ml}\boldsymbol{u}_{\bar{\tau} ml}(k\boldsymbol{r}) \tag{2.2}$$

where $f_{\tau ml}$ are the expansion coefficients or multipole moments and $\bar{\tau}$ denotes the complementary index. Here $\tau = 1$ ($\bar{\tau} = 2$) corresponds to a transversal electric (TE) wave and $\tau = 2$ ($\bar{\tau} = 1$) corresponds to a transversal magnetic (TM) wave. The other indices are $l = 1, 2, \ldots, \infty$ and $m = -l \ldots, l$ where l denotes the *order* of that mode. It can be shown that in the *far field* when $r \to \infty$, the electric field is given by

$$\boldsymbol{E}(\boldsymbol{r}) = \frac{\mathrm{e}^{-\mathrm{i}kr}}{kr}\boldsymbol{F}(\hat{\boldsymbol{r}}) \tag{2.3}$$

where $\boldsymbol{F}(\hat{\boldsymbol{r}})$ is the *far field amplitude* given by

$$\boldsymbol{F}(\hat{\boldsymbol{r}}) = \sum_{l=1}^{\infty}\sum_{m=-l}^{l}\sum_{\tau=1}^{2} \mathrm{i}^{l+2-\tau} f_{\tau ml}\boldsymbol{A}_{\tau ml}(\hat{\boldsymbol{r}}) \tag{2.4}$$

and where $\boldsymbol{A}_{\tau ml}(\hat{\boldsymbol{r}})$ are the *spherical vector harmonics* [1, 15, 24]. Furthermore, it can also be shown that the total power P_s transmitted by the antenna can be expressed in terms of the expansion coefficients as

$$P_s = \frac{1}{2\eta k^2}\sum_{l=1}^{\infty}\sum_{m=-l}^{l}\sum_{\tau=1}^{2} |f_{\tau ml}|^2. \tag{2.5}$$

For further details about the spherical vector mode representation we refer to the appendix and [1, 15, 24].

Next, we assume that the antenna(array) can be represented by a multiport model where a finite number of modes (multipoles) M is employed, see Fig. 1. Here,

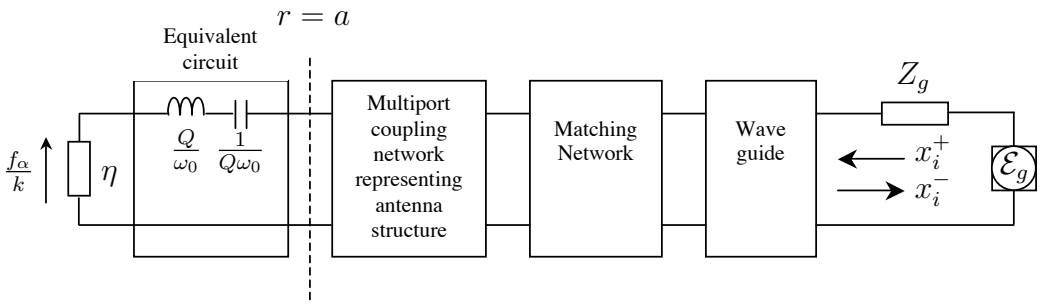

Figure 1: Multiport model of an arbitrary antenna inserted inside a sphere of radius $r = a$. The depicted series RCL resonance circuit is a Q factor approximation of the exact equivalent circuit of order l.

x_i^+ and x_i^- denote the incident and reflected voltages at the antenna waveguide connections for $i = 1, \ldots, N$ where N is the number of antenna ports. These voltages are normalized so that the power delivered to a particular antenna port is $\frac{|x_i^+|^2}{2Z_g}$ and the corresponding reflected power is $\frac{|x_i^-|^2}{2Z_g}$ where Z_g is the impedance of the propagating wave guide mode. Each antenna port is assumed to be connected to a lossless matching network as depicted in Fig. 1. In the left end of Fig. 1, we let the equivalent voltage $\frac{f_\alpha}{k}$ represent the propagated wave amplitude where f_α denotes the expansion coefficients for the spherical vector waves as in (2.1) and (2.5). Here, the multi-index $\alpha = (\tau, m, l)$ is chosen to simplify the notation.

On transmission from the input terminals with incident voltage waves x_i^+, the transmitted wave field f_α is given by

$$\left[\frac{f_\alpha}{k}\right] = \mathbf{S}\mathbf{x}^+\sqrt{\frac{\eta}{Z_g}} \tag{2.6}$$

where $\mathbf{S} = [S_{\alpha i}]$ is the properly scaled transmission matrix which maps the vector of incident voltages $\mathbf{x}^+ = [x_i^+]$ to propagated multipoles f_α. The reflected voltages are given by $\mathbf{x}^- = \mathbf{\Gamma}\mathbf{x}^+$ where $\mathbf{\Gamma}$ is the reflection matrix. Conservation of total power yields the relationship

$$\mathbf{\Gamma}^{\mathrm{H}}\mathbf{\Gamma} + \mathbf{S}^{\mathrm{H}}\mathbf{S} \leq \mathbf{I} \tag{2.7}$$

where equality holds for lossless antennas. Hence, we have for the singular values of these scattering matrices $\sigma(\mathbf{S}) \leq 1$ and $\sigma(\mathbf{\Gamma}) \leq 1$.

Now, considering one single incident wave x_i^+, the antenna reciprocity theorem [4] yields

$$x_i^- x_i^+ = -\mathrm{i}\frac{\lambda^2}{2\pi}\frac{Z_g}{\eta}\boldsymbol{F}(\hat{\boldsymbol{k}}_0)\cdot\boldsymbol{E}_0 \tag{2.8}$$

where $\boldsymbol{E}_0$ is the complex vector amplitude of an incoming plane wave $\boldsymbol{E}_0\mathrm{e}^{-\mathrm{i}k\hat{\boldsymbol{k}}_0\cdot\boldsymbol{r}}$ from direction $\hat{\boldsymbol{k}}_0$ and x_i^- the corresponding received signal. Further, $\boldsymbol{F}(\hat{\boldsymbol{r}})$ is the far field amplitude corresponding to the transmitted signal x_i^+. Hence, by using (2.4)

the received vector signal is obtained from the reciprocity theorem (2.8) as

$$\mathbf{x}^- = \sqrt{\frac{Z_g}{\eta}}\frac{2\pi}{k}\mathbf{TAE} \tag{2.9}$$

where $\mathbf{T} = \mathbf{S}^{\mathrm{T}} = [S_{i\alpha}]$, $\mathbf{A}$ is an $M \times 2$ matrix where each row corresponds to the spherical components of the spherical vector harmonics $\mathrm{i}^{l+1-\tau}\boldsymbol{A}_\alpha(\hat{\boldsymbol{k}}_0)$, and $\mathbf{E}$ is an 2×1 vector containing the corresponding signal components of the electric field $\boldsymbol{E}_0$. Observe that $\sigma(\mathbf{T}) \leq 1$.

Observe that the signal model given in (2.9) is in principle valid for *any* multiport antenna system. Given that we can calculate the farfield $\boldsymbol{F}(\hat{\boldsymbol{r}})$ from the incident voltage waves $\mathbf{x}^-$, the scattering matrix $\mathbf{T} = \mathbf{S}^{\mathrm{T}}$ is obtained by calculating the multipoles $f_\alpha = \mathrm{i}^{\tau-l-2}\int \boldsymbol{A}^*_{\tau ml}(\hat{\boldsymbol{r}}) \cdot \boldsymbol{F}(\hat{\boldsymbol{r}})\,\mathrm{d}\Omega$ by integrating over the unit sphere and by exploiting the orthonormality of the spherical vector harmonics.

As was originally described by Chu [2], an arbitrary antenna inside a sphere of radius $r = a$ can be modeled using a coupling network connecting independent equivalent circuits representing each spherical mode, see Fig. 1. The propagated power for each mode is represented by the power loss over the terminating resistance η and the wave impedance as seen by the spherical mode at radius a is equal to the input impedance of the equivalent circuit for all frequencies.

In theory, the equivalent circuits for the multipoles can be used to derive a Fano limit for any TE or TM mode. However, instead of using the analytic expressions of the impedance it is common to use the Q factor to get an estimate of the bandwidth [2, 3, 6, 7, 9, 10, 22, 29]. At and around the resonance frequency, ω_0, the antenna is modeled as a series RCL circuit as depicted in Fig. 1, and the impedance of the antenna is only matched to the feeding network at the resonance frequency. By considering an antenna of a given *electrical size* ka, *fractional bandwidth* B, and the Q factors which are computable for each mode order l [3], the Fano-theory [5] can be used to calculate the following upper bound for the transmission coefficient t_l for a particular mode, cf. e.g. [5, 8, 25, 26]

$$|t_l| \leq \sqrt{1 - \mathrm{e}^{-\frac{2\pi}{Q_l}\frac{1-B^2/4}{B}}}. \tag{2.10}$$

For all practical purposes the maximum useful order $l_{\max}$ is finite and can be coarsely estimated from (2.10) as follows. Suppose e.g. that we are only interested in the modes (τ, m, l) contributing to the far field with power $P_{\tau ml} \leq \varepsilon$. The maximum useful order $l_{\max}$ then satisfies

$$P_{\tau ml} = \frac{1}{2\eta k^2}|f_{\tau ml}|^2 \leq |t_l|^2 P_{\mathrm{in}} \leq \varepsilon \tag{2.11}$$

where P_{in} is the (appropriately scaled) input power.

Although any real multiport antenna may be analyzed using the signal model in (2.9), it is particulary interesting to investigate the fundamental physical limitations associated with a hypothetical ideal mode-coupled antenna for which there is no coupling between the antenna input terminals and the transmission matrix $\mathbf{T}$

contains the optimum transmission coefficients (2.10) on its main diagonal. Such an idealized antenna, even though it is not physically realizable, will constitute an important Benchmark for any real antenna system.

2.2 The Cramer-Rao Lower Bound for Polarization Estimation

Now, considering an array of J similar antennas modeled as in (2.9) and positioned at locations $\boldsymbol{r}_j$, a complex baseband model [30] for the received signal is given by

$$\mathbf{x} = \mathbf{V}\mathbf{E} + \mathbf{n} \tag{2.12}$$

where

$$\mathbf{V} = \sqrt{\frac{Z_g}{\eta}}\frac{2\pi}{k}\mathbf{a} \otimes \mathbf{T}\mathbf{A} \tag{2.13}$$

and where $\mathbf{a}$ is the $J \times 1$ *steering vector* of complex phases $\mathrm{e}^{-\mathrm{i}k\hat{\boldsymbol{k}}_0 \cdot \boldsymbol{r}_j}$ and $\otimes$ denotes the Kronecker product, cf. [30]. Further, the sensor noise $\mathbf{n}$ is modeled as zero mean white complex Gaussian noise [23] with variance σ_n^2 and covariance matrix $\sigma_n^2\mathbf{I}$. We assume a narrowband signal model where k corresponds to the carrier frequency ω_0 and the *fractional bandwidth* $B = \frac{\Delta\omega}{\omega_0}$ is reasonable low. Here $\Delta\omega$ denotes the absolute bandwidth and $\sigma_n^2 = N_0\omega_0 B$ where N_0 is the spectral density of the noise process. We consider a situation where the received electric field is partially polarized and the electric field $\mathbf{E}$ can be modeled as a zero mean complex Gaussian random process with covariance matrix

$$\mathbf{R} = \mathcal{E}\left\{\mathbf{E}\mathbf{E}^{\mathrm{H}}\right\} = \frac{1}{2}\begin{pmatrix} s_0 + s_1 & s_2 + \mathrm{i}s_3 \\ s_2 - \mathrm{i}s_3 & s_0 - s_1 \end{pmatrix} \tag{2.14}$$

where $\mathcal{E}$ denotes the expectation operator and s_0, s_1, s_2, s_3 denotes the Stoke's parameters [10]. We are interested in the estimation accuracy of the Stoke's polarization parameters[1] as well as the noise variance, which we write as a vector parameter $\boldsymbol{\xi} = [s_0 \; s_1 \; s_2 \; s_3 \; \sigma_n^2]^{\mathrm{T}}$. For our complex Gaussian case, the *Fisher information matrix* $\mathbf{I}(\boldsymbol{\xi})$ is given by [18]

$$[\mathbf{I}(\boldsymbol{\xi})]_{ij} = \mathrm{tr}\left\{\mathbf{C}^{-1}\frac{\partial \mathbf{C}}{\partial \xi_i}\mathbf{C}^{-1}\frac{\partial \mathbf{C}}{\partial \xi_j}\right\} \tag{2.15}$$

where $\mathbf{C}$ is the covariance matrix for the measurements, given by

$$\mathbf{C} = \mathcal{E}\left\{\mathbf{x}\mathbf{x}^{\mathrm{H}}\right\} = \mathbf{V}\mathbf{R}\mathbf{V}^{\mathrm{H}} + \sigma_n^2\mathbf{I}. \tag{2.16}$$

Now, it is readily verified that the expression (2.15) is invariant to an arbitrary phase scaling $\mathrm{e}^{\mathrm{i}\varphi_i}$ of the elements x_i of $\mathbf{x}$ in (2.12). Hence, with the ideal mode-coupled antenna, the Cramer Rao lower bound for estimating $\boldsymbol{\xi}$ is explicitely computable via the expressions (2.13) through (2.16) with the phase scaling $\mathrm{e}^{\mathrm{i}\varphi_i}$ chosen such that the optimum t_α in (2.10) are real, that is $t_\alpha = \sqrt{1 - \mathrm{e}^{-\frac{2\pi}{Q_l}\frac{1-B^2/4}{B}}}$.

[1] If we are interested also in the DOA parameters θ and ϕ, the model is straightforwardly extended with $\boldsymbol{\xi} = \left[\theta \; \phi \; s_0 \; s_1 \; s_2 \; s_3 \; \sigma_n^2\right]^{\mathrm{T}}$

3 Array Processing for Polarization Estimation

We introduce the concept of a probing multimode array with the purpose of estimating the state of polarization when the direction of arrival $\hat{\boldsymbol{k}}_0$ is given. Let $\mathbf{w}_i = \mathbf{C}_i^{-1}\mathbf{a}/\mathbf{a}^{\mathrm{H}}\mathbf{C}_i^{-1}\mathbf{a}$ be the weights of N independent Capon beamformers [30] where $\mathbf{a}$ is the steering vector corresponding to the given (probing) direction $\hat{\boldsymbol{k}}_0$, and $\mathbf{C}_i = \mathcal{E}\{\mathbf{x}_i\mathbf{x}_i^{\mathrm{H}}\}$ where $\mathbf{x}_i$ is the array input vector corresponding to a particular antenna mode i in (2.12). Here, $\mathbf{x}_i = \mathbf{V}_i\mathbf{E} + \mathbf{n}_i$ where $\mathbf{V}_i = \sqrt{\frac{Z_g}{\eta}}\frac{2\pi}{k}\mathbf{a} \otimes \mathbf{t}_i\mathbf{A}$ where $\mathbf{t}_i$ and $\mathbf{n}_i$ are the ith rows of $\mathbf{T}$ and $\mathbf{n}$, respectively.

It is readily seen that the signal model for the processed signals $\mathbf{y} = \left\{\mathbf{w}_i^{\mathrm{H}}\mathbf{x}_i\right\}$ becomes

$$\mathbf{y} = \mathbf{V}_0\mathbf{E} + \mathbf{n}_y \tag{3.1}$$

where $\mathbf{V}_0 = \sqrt{\frac{Z_g}{\eta}}\frac{2\pi}{k}\mathbf{TA}$ and $\mathbf{n}_y = \left\{\mathbf{w}_i^{\mathrm{H}}\mathbf{n}_i\right\}$, and where the covariance matrix is given by

$$\mathbf{C}_y = \mathbf{V}_0\mathbf{R}\mathbf{V}_0^{\mathrm{H}} + \sigma_n^2\mathbf{G} \tag{3.2}$$

where $\mathbf{G}$ is a diagonal matrix with diagonal entries $\mathbf{w}_i^{\mathrm{H}}\mathbf{w}_i$. Hence, it is assumed that the processor is able to reject a limited number (less then J) of interferers coming from discrete directions $\hat{\boldsymbol{k}}_j$, and the remaining noise is sensor noise colored by the processor weights.

The Maximum Likelihood (ML) estimator for the situation above can be derived by extending the results in e.g. [16, 30] which are given for the case when the noise is white and $\mathbf{G} = \mathbf{I}$. It is assumed here that the matrix $\mathbf{V} = \mathbf{V}_0$ has dimension $n \times m$ with $n > m$. Further, let $\widehat{\mathbf{R}}_y$ be the sample covariance matrix based on K independent measurements $\mathbf{y}_k$

$$\widehat{\mathbf{R}}_y = \frac{1}{K}\sum_{k=1}^{K}\mathbf{y}_k\mathbf{y}_k^H. \tag{3.3}$$

By extending the derivation in [30] to include a general positively definite coloration matrix $\mathbf{G}$ as above, the ML estimator for $(\mathbf{R}, \sigma_n^2)$ can be found as

$$\hat{\sigma}_n^2 = \frac{1}{n-m}\mathrm{tr}\mathbf{G}^{-1}\mathbf{P}_V^{\perp}\widehat{\mathbf{R}}_y \tag{3.4}$$

$$\widehat{\mathbf{R}} = \mathbf{V}^{+}\left(\widehat{\mathbf{R}}_y - \hat{\sigma}_n^2\mathbf{G}\right)(\mathbf{V}^{+})^H \tag{3.5}$$

where

$$\mathbf{P}_V^{\perp} = \mathbf{I} - \mathbf{V}\left(\mathbf{V}^H\mathbf{G}^{-1}\mathbf{V}\right)^{-1}\mathbf{V}^H\mathbf{G}^{-1} \tag{3.6}$$

$$\mathbf{V}^{+} = \left(\mathbf{V}^H\mathbf{G}^{-1}\mathbf{V}\right)^{-1}\mathbf{V}^H\mathbf{G}^{-1} \tag{3.7}$$

are the orthogonal projector onto $\{\mathcal{R}\{\mathbf{V}\}\}^{\perp}$ and the pseudoinverse of $\mathbf{V}$, respectively, where the weighted norm based on $\mathbf{G}^{-1}$ is used.

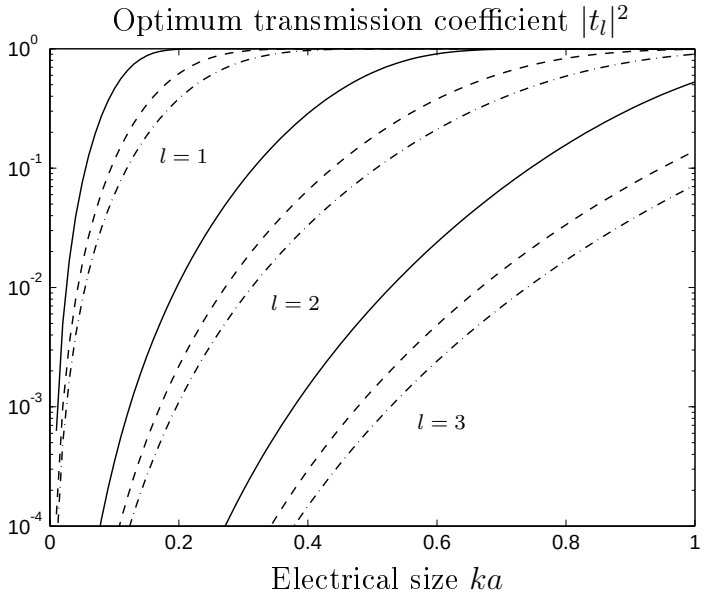

Figure 2: Optimum transmission coefficient $|t_l|^2$ as a function of electrical size ka for the first 3 mode orders $l = 1, 2, 3$. Fractional bandwidth is $B = 1, 5, 10$ %.

4 Numerical examples

In Fig. 2 is shown the optimum transmission coefficients $|t_l|^2$ from (2.10) with Q factors corresponding to the first 3 mode orders $l = 1, 2, 3$, cf. [3], as the electrical size ka as well as the fractional bandwidth B is varied. The figure illustrates the difficulty to match higher order modes, as well as the fact that all modes will ultimately become useful (useless) as the electrical size increases (decreases), or as the bandwidth decreases (increases).

Consider now a single, ideal tripole antenna with $\mathbf{a} = 1$ and

$$\mathbf{A} = \sqrt{\frac{3}{8\pi}} \begin{pmatrix} \cos\theta\cos\phi & -\sin\phi \\ \cos\theta\sin\phi & \cos\phi \\ -\sin\theta & 0 \end{pmatrix} \tag{4.1}$$

corresponding to the three fundamental TM modes of lowest order $l = 1$, or equivalently, the three ideal electrical dipoles in the cartesian base vector directions $\hat{\boldsymbol{x}}, \hat{\boldsymbol{y}}, \hat{\boldsymbol{z}}$.

In Fig. 3 is shown the Cramer-Rao bound for the polarization parameters s_0, s_1, s_2 and s_3 versus electrical size ka. The diagonal elements of $\mathbf{I}^{-1}(\boldsymbol{\xi})$ are based on (2.15) with the optimum transmission coefficients t_α calculated as in (2.10) with $B = 5$ % and $Q = \frac{1}{ka} + \frac{1}{(ka)^3}$, cf. [3]. The Stoke's parameters are parameterized as

$$\begin{aligned} s_1 &= P s_0 \cos(2\alpha)\cos(2\beta) \\ s_2 &= P s_0 \cos(2\alpha)\sin(2\beta) \\ s_3 &= P s_0 \sin(2\alpha) \end{aligned} \tag{4.2}$$

where $0 \leq P \leq 1$ is the *degree of polarization*. The signal-to-noise ratio is defined as $\text{SNR} = \frac{s_0}{\sigma_n^2}\frac{Z_g}{\eta}(\frac{2\pi}{k})^2$ and was chosen to 50 dB. In this example we have chosen a

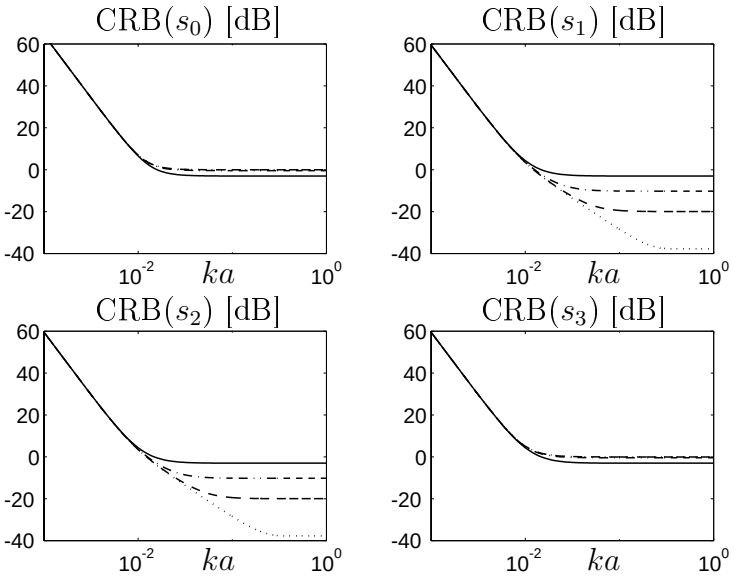

Figure 3: Cramer-Rao bound for the polarization parameters s_0, s_1, s_2 and s_3 versus electrical size ka. Circular polarization with $s_0 = 1$, $s_1 = 0$, $s_2 = 0$ and $s_3 = 1$. The solid, dashed-dotted, dashed and dotted lines correspond to $P = 0$, 0.9, 0.99 and 1, respectively. SNR is 50 dB and $B = 5\%$.

situation with circular polarization with $s_0 = 1$, $s_1 = 0$, $s_2 = 0$ and $s_3 = 1$. The solid, dashed-dotted, dashed and dotted lines correspond to $P = 0$, 0.9, 0.99 and 1, respectively. The result in Fig. 3 is invariant to the directional parameters θ and ϕ but depends strongly on polarization. In particular, only s_1 and s_2 can be efficiently estimated in this example, and the performance improves drastically as the degree of polarization P approaches unity.

Although the result above should be expected, it can be better understood by performing a principal parameter analysis. We define the principal parameters $\boldsymbol{\eta}$ to be the linear transformation

$$\boldsymbol{\eta} = \mathbf{U}^{\mathrm{H}}\boldsymbol{\xi} \tag{4.3}$$

where $\mathbf{U}$ are the left singular vectors from the Singular Value Decomposition (SVD) of the Fisher information, $\mathbf{I}(\boldsymbol{\xi}) = \mathbf{U}\boldsymbol{\Sigma}\mathbf{V}^{\mathrm{H}}$. The principal parameters η_i are uncoupled, and their corresponding Cramer-Rao bounds are the reciprocal of the singular values σ_i^{-1}.

Fig. 4 a) shows the Cramer-Rao bounds σ_i^{-1} for the principal parameters η_i, as well as $-\log\det\mathbf{I}$ plotted as a function of the degree of polarization P. Fig. 4 b) shows the corresponding results for the original parameters ξ_i. The parameter situation is the same as above, except now SNR is 30 dB and $ka = 1$.

Note that the performance results for the principal parameters in Fig. 4 a) are invariant not only to the directional parameters θ and ϕ, but are also invariant to the polarization parameters α and β. In other words, the performance of the principal parameters η_i depends only on the degree of polarization P, whereas the

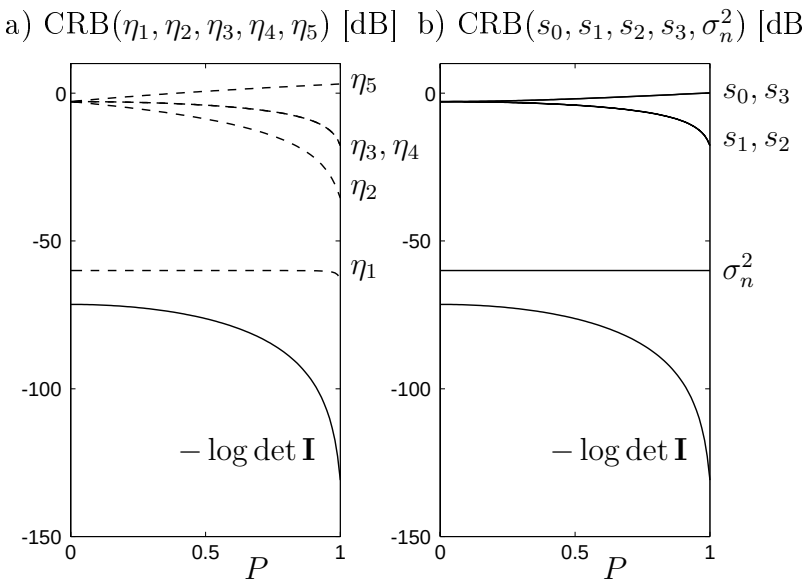

Figure 4: a) Cramer-Rao bound for the principal parameters $\eta_1, \eta_2, \eta_3, \eta_4, \eta_5$ versus degree of polarization P. b) Cramer-Rao bound for the polarization parameters s_0, s_1, s_2, s_3 and σ_n^2 versus degree of polarization P. Circular polarization with $s_0 = 1$, $s_1 = 0$, $s_2 = 0$ and $s_3 = 1$. SNR is 30 dB, $ka = 1$ and $B = 5\%$.

performance of the original parameters ξ_i depends also on the actual situation with polarization parameters α and β.

In this example situation with circular polarization, it is concluded that the relevant parameters to measure are s_1 and s_2 whereas s_0 and s_3 cannot be measured as efficiently. By studying the left singular vectors in $\mathbf{U}$ which are plotted in Fig. 5 for $P = 1$, we can identify the principal parameters as linear combinations of the original parameters. The "best" parameter η_1 corresponds directly to the noise parameter σ_n^2 which is thus a relevant parameter to measure. Further, $\eta_2 \sim s_3 - s_0$ and $\eta_5 \sim s_3 + s_0$ are "good" and "poor" parameters to estimate, respectively. It is furthermore "appropriate" to estimate s_1 and s_2 since (s_1, s_2) belongs to the subspace spanned by the singular vectors corresponding to the two principal parameters η_3 and η_4 sharing the same singular value (and hence the same Cramer-Rao bound). It should also be noted that the SVD produces here a decomposition which has a direct physical significance. Thus, $\eta_2 \sim s_3 - s_0$ and $\eta_5 \sim s_3 + s_0$ correspond also to the power in the left and right circularly polarized components, respectively, see e.g. [24]. Hence, given that the wave is right circularly polarized (as in our example), the (absolute) performance of estimating the power of a weak left circularly polarized signal component is much better than for estimating the power of the dominating right circularly polarized signal component.

In conclusion, the study shows that the estimation performance of the tripole antenna as measured by the functional $\log\det\mathbf{I}(\boldsymbol{\xi})$ is invariant to the directional parameters θ and ϕ as well as to the polarization parameters α and β. However, the functional $\log\det\mathbf{I}(\boldsymbol{\xi})$ depends strongly on the degree of polarization P, as well

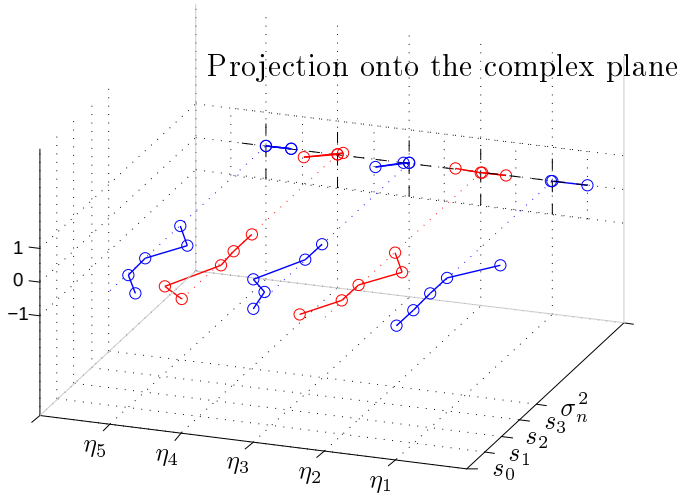

Figure 5: Visualization of the complex left singular vectors in $\mathbf{U}$ showing the linear dependence between the original $(s_0, s_1, s_2, s_3, \sigma_n^2)$ and principal $(\eta_1, \eta_2, \eta_3, \eta_4, \eta_5)$ parameters. Circular polarization with $s_0 = 1$, $s_1 = 0$, $s_2 = 0$, $s_3 = 1$ and $P = 1$. SNR is 30 dB, $ka = 1$ and $B = 5\%$.

as on the electrical size ka of the antenna and the bandwidth B of the system. The principal parameter analysis is a useful technique to investigate the significance of different parameters.

5 Summary

Fundamental physical limitations associated with polarization and/or DOA estimation using antennas or antenna arrays are analyzed. By using spherical vector modes as a generic model for the scattering, we show how the corresponding Cramer-Rao lower bounds can be calculated for any real antenna system. The spherical vector modes and their associated equivalent circuits and Q factor approximations are used together with the broadband Fano theory as a general framework for analyzing electrically small multiport antennas. The concept of a probing multimode array is introduced which is equivalent to one single multimode antenna without interferers but with colored noise, and the explicit form of the corresponding ML estimator for the state of polarization is given. A principal parameter analysis using the SVD of the Fisher information matrix is employed to evaluate the performance of the ideal multimode antenna processor with respect to its ability to estimate the state of polarization of a partially polarized plane wave coming from a given direction. Our study shows that the estimation performance of the ideal multimode antenna is invariant to the directional parameters as well as to the polarization parameters for a given degree of polarization. However, the estimation performance depends

strongly on the degree of polarization, as well as on the electrical size of the antenna and the bandwidth of the system.

Appendix A Spherical Vector Waves

The outgoing spherical vector waves are given by

$$\begin{aligned}
&\boldsymbol{u}_{1ml}(k\boldsymbol{r}) = \mathrm{h}_l^{(2)}(kr)\boldsymbol{A}_{1ml}(\hat{\boldsymbol{r}}) \\
&\boldsymbol{u}_{2ml}(k\boldsymbol{r}) = \frac{1}{k}\nabla \times \boldsymbol{u}_{1ml}(k\boldsymbol{r}) = \\
&\frac{(kr\mathrm{h}_l^{(2)}(kr))'}{kr}\boldsymbol{A}_{2ml}(\hat{\boldsymbol{r}}) + \sqrt{l(l+1)}\frac{\mathrm{h}_l^{(2)}(kr)}{kr}\boldsymbol{A}_{3ml}(\hat{\boldsymbol{r}})
\end{aligned} \tag{A.1}$$

where $\boldsymbol{A}_{\tau ml}(\hat{\boldsymbol{r}})$ are the *spherical vector harmonics* and $\mathrm{h}_l^{(2)}(x)$ the *spherical Hankel functions of the second kind*, see [1, 15, 24]. The spherical vector harmonics $\boldsymbol{A}_{\tau ml}(\hat{\boldsymbol{r}})$ are given by

$$\begin{aligned}
\boldsymbol{A}_{1ml}(\hat{\boldsymbol{r}}) &= \frac{1}{\sqrt{l(l+1)}}\nabla \times (\boldsymbol{r}\mathrm{Y}_{ml}(\hat{\boldsymbol{r}})) \\
\boldsymbol{A}_{2ml}(\hat{\boldsymbol{r}}) &= \hat{\boldsymbol{r}} \times \boldsymbol{A}_{1ml}(\hat{\boldsymbol{r}}) \\
\boldsymbol{A}_{3ml}(\hat{\boldsymbol{r}}) &= \hat{\boldsymbol{r}}\mathrm{Y}_{ml}(\hat{\boldsymbol{r}})
\end{aligned} \tag{A.2}$$

where $\mathrm{Y}_{ml}(\hat{\boldsymbol{r}})$ are the scalar *spherical harmonics* given by

$$\mathrm{Y}_{ml}(\theta,\phi) = (-1)^m\sqrt{\frac{2l+1}{4\pi}}\sqrt{\frac{(l-m)!}{(l+m)!}}\mathrm{P}_l^m(\cos\theta)\mathrm{e}^{\mathrm{i}m\phi} \tag{A.3}$$

and where $\mathrm{P}_l^m(x)$ are the *associated Legendre functions* [1]. For negative m-indices, the scalar waves satisfies the symmetry $\mathrm{Y}_{-m,l}(\hat{\boldsymbol{r}}) = (-1)^m\mathrm{Y}_{ml}^*(\hat{\boldsymbol{r}})$, and hence

$$\boldsymbol{A}_{\tau,-m,l}(\hat{\boldsymbol{r}}) = (-1)^m\boldsymbol{A}_{\tau ml}^*(\hat{\boldsymbol{r}}). \tag{A.4}$$

References

[1] G. B. Arfken and H. J. Weber. *Mathematical Methods for Physicists.* Academic Press, New York, fifth edition, 2001.

[2] L. J. Chu. Physical limitations of Omni-Directional antennas. *Appl. Phys.*, **19**, 1163–1175, 1948.

[3] R. E. Collin and S. Rothschild. Evaluation of antenna Q. *IEEE Trans. Antennas Propagat.*, **12**, 23–27, January 1964.

[4] S. Drabowitch, A. Papiernik, H. Griffiths, J. Encinas, and B. L. Smith. *Modern Antennas.* Chapman & Hall, 1998.

[5] R. M. Fano. Theoretical limitations on the broadband matching of arbitrary impedances. *Journal of the Franklin Institute*, **249**(1,2), 57–83 and 139–154, 1950.

[6] R. L. Fante. Quality factor of general antennas. *IEEE Trans. Antennas Propagat.*, **17**(2), 151–155, March 1969.

[7] W. Geyi, P. Jarmuszewski, and Y. Qi. The Foster reactance theorem for antennas and radiation Q. *IEEE Trans. Antennas Propagat.*, **48**(3), 401–408, March 2000.

[8] M. Gustafsson and S. Nordebo. On the spectral efficiency of a sphere. Technical Report LUTEDX/(TEAT-7127)/1–24/(2004), Lund Institute of Technology, Department of Electroscience, P.O. Box 118, S-211 00 Lund, Sweden, 2004. `http://www.es.lth.se/teorel`.

[9] R. C. Hansen. Fundamental limitations in antennas. *Proc. IEEE*, **69**(2), 170–182, 1981.

[10] R. F. Harrington. *Time Harmonic Electromagnetic Fields.* McGraw-Hill, New York, 1961.

[11] K.-C. Ho, K.-C. Tan, and A. Nehorai. Estimating directions of arrival of completely and incompletely polarized signals with electromagnetic vector sensors. *IEEE Trans. Signal Process.*, **47**(10), 2845–2852, October 1999.

[12] K.-C. Ho, K.-C. Tan, and B. T. G. Tan. Efficient method for estimating directions–of–arrival of partially polarized signals with electromagnetic vector sensors. *IEEE Trans. Signal Process.*, **45**(10), 2485–2498, October 1997.

[13] K.-C. Ho, K.-C. Tan, and B. T. G. Tan. Linear dependence of steering vectors associated with tripole arrays. *IEEE Trans. Antennas Propagat.*, **46**(11), 1705–1711, November 1998.

[14] B. Hochwald and A. Nehorai. Polarimetric modeling and parameter estimation with applications to remote sensing. *IEEE Trans. Signal Process.*, **43**(8), 1923–1935, August 1995.

[15] J. D. Jackson. *Classical Electrodynamics.* John Wiley & Sons, New York, second edition, 1975.

[16] A. G. Jaffer. Maximum likelihood direction finding of stochastic sources: A separable solution. In *1988 IEEE International Conference on Acoustics, Speech, and Signal Processing*, pages 2893–2896. IEEE Signal Processing Society, 1988.

[17] A. Karlsson. Physical limitations of antennas in a lossy medium. *IEEE Trans. Antennas Propagat.*, **52**, 2027–2033, 2004.

[18] S. M. Kay. *Fundamentals of Statistical Signal Processing, Estimation Theory.* Prentice-Hall, Inc., NJ, 1993.

[19] H. Krim and M. Viberg. Two decades of array signal processing research: the parametric approach. *IEEE Signal Processing Magazine*, **13**(4), 67–94, July 1996.

[20] J. Li. Direction and polarization estimation using arrays with small loops and short dipoles. *IEEE Trans. Antennas Propagat.*, **41**(3), 379–387, March 1993.

[21] J. Li and P. Stoica. Efficient parameter estimation of partially polarized electromagnetic waves. *IEEE Trans. Signal Process.*, **42**(11), 3114–3125, November 1994.

[22] J. S. McLean. A re-examination of the fundamental limits on the radiation Q of electrically small antennas. *IEEE Trans. Antennas Propagat.*, **44**(5), 672–676, May 1996.

[23] K. S. Miller. *Complex Stochastic Processes.* Addison–Wesley Publishing Company, Inc., 1974.

[24] R. G. Newton. *Scattering Theory of Waves and Particles.* Dover Publications, New York, second edition, 2002.

[25] S. Nordebo and M. Gustafsson. Fundamental limitations for DOA estimation by a sphere. Technical Report LUTEDX/(TEAT-7128)/1–26/(2004), www.es.lth.se/teorel/, Lund Institute of Technology, Department of Electroscience, P.O. Box 118, S-211 00 Lund, Sweden, 2004.

[26] S. Nordebo and M. Gustafsson. Multichannel broadband Fano theory for arbitrary lossless antennas with applications in DOA estimation. In *2005 IEEE International Conference on Acoustics, Speech, and Signal Processing*, volume IV, pages 969–972, 2005.

[27] P. Stoica and A. Nehorai. MUSIC, maximum likelihood, and Cramer-Rao bound: further results and comparisons. *IEEE Trans. Signal Process.*, **38**(12), 2140–2150, December 1990.

[28] A. Swindlehurst and M. Viberg. Subspace fitting with diversely polarized antenna arrays. *IEEE Trans. Antennas Propagat.*, **41**(12), 1687–1694, December 1993.

[29] H. L. Thal. Exact circuit analysis of spherical waves. *IEEE Trans. Antennas Propagat.*, **26**(2), 282–287, March 1978.

[30] H. L. V. Trees. *Optimum Array Processing.* John Wiley & Sons, Inc., New York, 2002.

[31] M. Viberg, P. Stoica, and B. Ottersten. Maximum likelihood array processing in spatially correlated noise fields using parameterized signals. *IEEE Trans. Signal Process.*, **45**(4), 996–1004, April 1997.

[32] A. J. Weiss and B. Friedlander. Maximum likelihood signal estimation for polarization sensitive arrays. *IEEE Trans. Antennas Propagat.*, **41**(7), 918–925, July 1993.

[33] K. T. Wong. Direction finding/polarization estimation – dipole and/or loop triad(s). *IEEE Transactions on Aerospace and Electronic Systems*, **37**(2), 679–684, April 2001.

[34] K. T. Wong, L. Li, and M. D. Zoltowski. Root–MUSIC–based direction–finding and polarization estimation using diversely polarized possibly collocated antennas. *IEEE Antennas & Wireless Propagation Letters*, **3**(8), 129–132, 2004.

[35] K. T. Wong and M. D. Zoltowski. Closed–form direction finding and polarization estimation with arbitrarily spaced electromagnetic vector–sensors at unknown locations. *IEEE Trans. Antennas Propagat.*, **48**(5), 671–681, May 2000.